Journal of Engineering Sciences
Assiut University
Faculty of Engineering
Vol. 44
No. 6
November 2016
PP. 675 – 689

# DEVELOPMENT OF STEEL FIBER-REINFORCED SELF-CONSOLIDATING CONCRETE FOR REPAIRING PURPOSES

**Yehia. A. Hassanean, Mohammed M. Ahmed, Kamal Abas Assaf, Amr E. M. Abdallah**

*Civil Engineering Department, Assiut University, Assiut, Egypt.*

Received 7 August 2016; Accepted 31 September 2016

## ABSTRACT

Fifteen self-consolidating concrete (SCC) as well as five steel fiber-reinforced self-consolidating concrete (SFR-SCC) mixes using full-length crimped steel fibers were developed and tested in order to optimize a suitable (SFR-SCC) mix for repair of beams. Water-cementitious materials (w/cm) ratio, sand/coarse aggregate ratio and presence of basalt dust were the main variables taken into consideration. The test results showed that the mix design for the SCC mixes without steel fibers can be achieved by satisfying the flowability criterion. But for the design of self-consolidating concrete mixes with steel fibers, both the flowability and passing ability criteria must be satisfied. Basalt dust was found to be necessary for SCC mixes without fibers with sand/coarse aggregate ratios of 0.9 and 0.8, and also for developing SCC mixes with crimped steel fibers. SFR-SCC mix with sand/coarse aggregate of 1.1 had satisfactory results in both fresh and hardened properties. SFR-SCC mixes with sand/coarse aggregate of 0.9 and 0.8 did not satisfy fresh properties criteria even with dust/coarse aggregate ratio of 0.4. The suggested SFR-SCC mix was used to repair a beam cracked due to shear stresses. For this purpose, two RC beams were cast and tested under three-point loading. One beam was tested as control beam and the other beam was repaired using the suggested mix. The inclined cracking and ultimate load of the repaired beam were increased by 87.5% and 91% comparing to the control beam, respectively. The flexural stiffness was increased significantly for the repaired beam comparing to the control beam. The test results also showed the great contribution of SFR-SCC in both compression and tension zones.

***Keywords:*** full-length crimped steel fibers, self-consolidating concrete, steel fiber-reinforced self-consolidating concrete, shear repairing.

## 1. Introduction

The ideal design of self-consolidating concrete (SCC) is the balance between the requirements of flowability and stability to fill the formwork without need for compaction and to avoid segregation during casting or flowing through narrow openings and congested reinforcement, respectively. The flowability of SCC can be achieved using high range water reducing admixtures (HRWRA). The stability of SCC can be obtained by balancing the of aggregate and paste volumes in the mix, choosing cement and cement replacement materials (CRM) or supplementary cementitious materials (SCM) quantities and types, and using viscosity modifying admixtures (VMA) if necessary [9]. Adding steel fibers promotes the mechanical properties of SCC as it does to conventional concrete. However, the addition of fibers compromises the workability of concrete because of its large aspect ratio, large surface

area and crimped profile. The limit of steel fibers dosage depends on fiber shape and the mixing proportions of SCC. Acceptable workability of SCC requires fibers to be homogenously distributed in the mix without clumping and well-encapsulated by mortar [5].

The aim of this study is to develop steel fiber-reinforced self-consolidating concrete (SFR-SCC) mixes using the locally-available materials and full-length crimped steel fibers. This study investigates the effect of mixing proportions on fresh as well as hardened properties of SCC and SFR-SCC. A suitable SFR-SCC for repairing beams cracked due to shear stresses is developed.

## 2. Experimental program

An intensive experimental program was carried out in order to develop a highly flowable and non-segregating SFR-SCC mix. For this purpose, fifteen non-fibrous SCC mixes were cast and tested to study the effect of the constituent materials on the self-consolidating behavior. And also to adjust the suitable w/cm ratio for mixing without need for retarding admixtures. Then five SFR-SCC mixes were cast and tested in order to select a suitable mix for the repairing process. A target slump flow ranged between 600 to 650 mm was initially set as well as a target compressive strength of 600 kg/cm$^2$. The used materials were natural sand, crushed basalt with a maximum size of 9.5 mm, basalt dust (particle size range 0.05- 4 mm) was used in some mixes as a filler and to increase the paste volume to lubricate the coarse aggregate and steel fibers [3], TYPE I cement with a grade of 32.5 N was used as it gave the best results among various locally-available types of cement, as determined from preliminary tests on trial mixes as will be discussed later. Also, silica fume was used as a supplementary cementitious material (SCM). The chemical composition of the used cement and silica fume as resulted from tests conducted by CEMEX Egypt as well as their physical properties are listed in Table 1. A modified Polycarboxylates – based HRWRA was used. Also, full – length crimped steel fibers with length of 35 mm, aspect ratio of 50 and tensile strength of 6500 kg/cm$^2$ were used.

### *2.1. Non-fibrous SCC mixes*

Non-fibrous SCC mixes were developed with constant cement content of 500 kg/m$^3$. Also, silica fume content was fixed at 75 kg/m$^3$. For each w/cm ratio, a wide range of sand/ coarse aggregate ratios was tested as suggested by many researchers [1, 3, 4]. Sand/ coarse aggregate ratios of 0.8, 0.9, 1.0, 1.1, and 1.2 were tested. Basalt dust was necessary for mixes with 0.8 and 0.9 sand/ coarse aggregate ratios at low w/cm ratios in order to provide a sufficient amount of paste to encapsulate the coarse aggregate [3]. HRWRA content was adjusted for each sand/ coarse aggregate and w/cm ratio in order to achieve the desired fresh properties for the mix. Table 2 shows the mixing proportions for non-fibrous SCC mixes. A laboratory pan mixer with maximum capacity of 100 liter was used according to the mixing procedure shown in Fig. 1.a [6]. Slump flow test, T500 test, VSI test, L-box test, V-funnel test and column segregation test were conducted for each mix to evaluate its fresh properties (Fig. 2). Also, 15×15×15 cm cubes were cast for each mixture to evaluate its compressive strength.

### *2.2. SFR-SCC mixes*

To develop SFR-SCC mixes, w/cm ratio was fixed at 0.35 to be used with no need to retarders. It was found that silica fume needed to increase to 90 kg/m$^3$ in order to achieve the target slump flow with presence of steel fibers. For all mixes, steel fiber volume fraction (Vf %) was fixed at 0.75% as recommended by some researchers for repairing

**Table 1.**
Chemical composition and physical properties of the used cement and silica fume

| Property | Type I cement | Silica fume |
|---|---|---|
| SiO2 (%) | 21.0 | 86.07 |
| Al2O3 (%) | 6.1 | 1.03 |
| Fe2O3 (%) | 3.0 | 3.39 |
| CaO (%) | 61.5 | 0.55 |
| MgO (%) | 3.8 | 2.52 |
| SO3 (%) | 2.5 | - |
| $Na_2O$ | 0.4 | 0.21 |
| $K_2O$ | 0.3 | 0.99 |
| $Mn_2O_3$ | - | 0.12 |
| $TiO_2$ | - | 0.2 |
| $P_2O_5$ | - | - |
| $Cr_2O_3$ | - | 0.02 |
| CI (%) | - | - |
| $C_3A$ (%) | - | - |
| Dissolved impurities (%) | - | - |
| L.O.I. (%) | 1.4 | 3.50 |
| Specific gravity | 3.15 | 2.0 |
| Initial setting (min) | 90 | - |
| Final setting (min) | 285 | - |
| Fineness ($cm^2$/gm) | 2870 | - |

**Table 2.**
Mixing proportions for tested mixes.

| Mixture type | Mixture No. | Sand/coarse Aggregate | w/cm | Cement ($kg/m^3$) | Silica Fume ($kg/m^3$) | Sand ($kg/m^3$) | Basalt ($kg/m^3$) | Dust ($kg/m^3$) | HRWRA ($kg/m^3$) | $V_f$% |
|---|---|---|---|---|---|---|---|---|---|---|
| SCC | 1 | 1.2 | 0.4 | 500 | 75 | 804 | 670 | 0 | 4.67 | - |
| | 2 | 1.1 | 0.4 | 500 | 75 | 773 | 703 | 0 | 4.5 | - |
| | 3 | 1.0 | 0.4 | 500 | 75 | 740 | 740 | 0 | 4.4 | - |
| | 4 | 0.9 | 0.4 | 500 | 75 | 703 | 781 | 0 | 3.72 | - |
| | 5 | 0.8 | 0.4 | 500 | 75 | 661 | 826 | 0 | 3.55 | - |
| | 6 | 1.2 | 0.38 | 500 | 75 | 818 | 682 | 0 | 6.25 | - |
| | 7 | 1.1 | 0.38 | 500 | 75 | 788 | 717 | 0 | 5.07 | - |
| | 8 | 1.0 | 0.38 | 500 | 75 | 753 | 753 | 0 | 6.08 | - |
| | 9 | 0.9 | 0.38 | 500 | 75 | 716 | 795 | 0 | 4.73 | - |
| | 10 | 0.8 | 0.38 | 500 | 75 | 673 | 842 | 0 | 4.56 | - |
| | 11 | 1.2 | 0.35 | 500 | 75 | 836 | 697 | 0 | 10.8 | - |
| | 12 | 1.1 | 0.35 | 500 | 75 | 805 | 732 | 0 | 10.64 | - |
| | 13 | 1.0 | 0.35 | 500 | 75 | 772 | 772 | 0 | 8.45 | - |
| | 14 | 0.9 | 0.35 | 500 | 75 | 651 | 724 | 181 | 12.84 | - |
| | 15 | 0.8 | 0.35 | 500 | 75 | 609 | 761 | 190 | 12.7 | - |
| SFR-SCC | 16 | 1.2 | 0.35 | 500 | 90 | 743 | 619 | 155 | 11.2 | 0.75 |
| | 17 | 1.1 | 0.35 | 500 | 90 | 711 | 646 | 162 | 11 | 0.75 |
| | 18 | 1.0 | 0.35 | 500 | 90 | 678 | 678 | 170 | 9.87 | 0.75 |
| | 19 | 0.9 | 0.35 | 500 | 90 | 601 | 667 | 267 | 10.86 | 0.75 |
| | 20 | 0.8 | 0.35 | 500 | 90 | 560 | 700 | 280 | 11.18 | 0.75 |

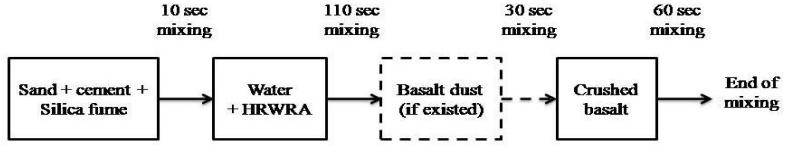


**Fig. 1.a.** Mixing procedure for non – fibrous SCC mixes.

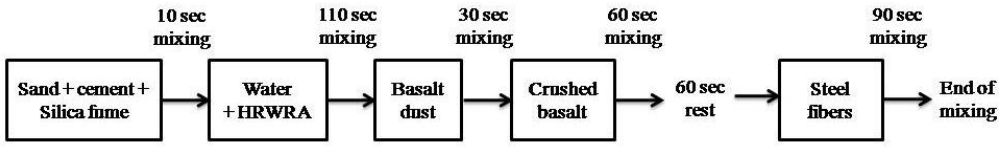


**Fig. 1.b.** Mixing procedure for SFR-SCC mixes.

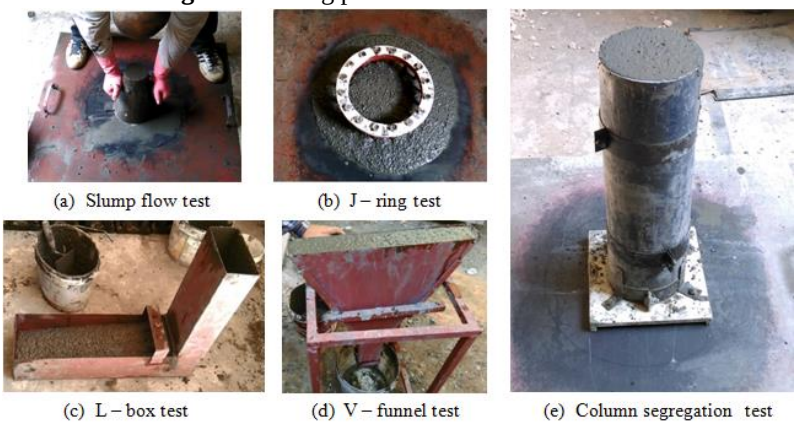


**Fig. 2.** Testing mixes for fresh properties.

purposes [4], while dust/ coarse aggregate ratio varied between 0.25 and 0.4. For each mix, the amount of fibers added was accompanied by a reduction of coarse aggregate only by the same absolute volume [8]. HRWRA content was adjusted for each sand/ coarse aggregate ratio in order to achieve the desired fresh properties for the mix. Table 2 shows the mixing proportions SFR-SCC mixes and Fig. 1.b shows the mixing procedure [6]. Also, slump flow test, T500 test, VSI test, J-ring test, V-funnel test and column segregation test were conducted for each mix to evaluate its fresh properties (Fig. 2). Also, mixes 16, 17, 18, and 19 were developed using other types of cement such as TYPE I cement with a grade of 42.5 N and TYPE II cement with a grade of 52.5 N. This was done in order to evaluate the efficiency of the various types of cement in terms of fresh and hardened properties. For each mix, 15×15×15 cm cubes as well as 15×30 cm cylinders were cast to evaluate its compressive and tensile strength, respectively. The cubes were tested under axial compression while the cylinders were tested under indirect tension. Both tests were conducted using a hydraulic machine with digital display with 150 tons load capacity.

## 3. Results and discussion

The intensive experimental program carried out in this study gave a lot of data to be analyzed and discussed as follows.

### *3.1. Non-fibrous SCC mixes*

Initiating the experimental program with developing non-fibrous SCC mixes was to study the self-consolidating behavior of the concrete using the available materials prior to adding steel fibers. The fresh properties as well as compressive strength of SCC mixes are presented in Table 3. The investigation of Figs. 3.a and 3.b shows that sand/coarse aggregate ratio has the same trend effect on both the slump flow and $h_2/h_1$ ratio except for mixes with sand/coarse aggregate ratio of 0.8 at w/cm of 0.38 and 0.35. Figs. 3.d, 3.e and 3.c show that v-funnel test results are better correlated with column segregation's than T500's. These correlations can ensure that satisfaction of flowability criteria is sufficient for the mix design

of non-fibrous SCC. Fig. 3.e shows the direct proportion between segregation% and w/cm ratio. The large drops between segregation percentages of mixes 9 and 14 as well as 10 and 15 are primarily due to the utilization of basalt dust which noticeably enhanced the stability of the mixes. Fig. 4.m shows an earlier version of mix 14 before adding basalt dust. Clear segregation of coarse aggregate can be noticed as the stability of the mix is compromised due to lack of the mortar. Figs. 4 and 5 shows all mixes under slump flow as well as L-box test.

**Table 3.**
Test results for tested mixes.

| Mixture type | Mixture No. | Slump flow (mm) | L – box $h_2/h_1$ | J – ring flow (mm) | VSI | T500 (sec) | $t_v$ (sec) | S% | $f_{cu}$ (kg/cm²) | $f_{ct}$ (kg/cm²) |
|---|---|---|---|---|---|---|---|---|---|---|
| SCC | 1 | 710 | 0.9 | - | 1 | 2.9 | 6.5 | 2.89 | 515.1 | - |
| | 2 | 695 | 0.81 | - | 1 | 2.5 | 6.3 | 3.23 | 547.8 | - |
| | 3 | 610 | 0.8 | - | 1 | 2.3 | 6.0 | 4.46 | 546.2 | - |
| | 4 | 685 | 0.82 | - | 0 | 2.5 | 6.0 | 5.55 | 581.8 | - |
| | 5 | 635 | 0.8 | - | 1 | 2.3 | 5.8 | 6.32 | 575.1 | - |
| | 6 | 650 | 0.8 | - | 0 | 2.3 | 6.8 | 2.15 | 610.9 | - |
| | 7 | 680 | 0.84 | - | 0 | 2.4 | 6.5 | 3.18 | 623.0 | - |
| | 8 | 710 | 0.875 | - | 0 | 2.7 | 6.4 | 3.93 | 585.8 | - |
| | 9 | 660 | 0.84 | - | 1 | 2.3 | 6.3 | 5.33 | 639.0 | - |
| | 10 | 715 | 0.86 | - | 1 | 2.2 | 5.9 | 6.15 | 646.1 | - |
| | 11 | 700 | 0.97 | - | 0 | 2.8 | 7.2 | 1.12 | 632.1 | - |
| | 12 | 680 | 0.93 | - | 0 | 2.9 | 6.9 | 2.66 | 641.1 | - |
| | 13 | 675 | 0.93 | - | 1 | 2.8 | 6.7 | 3.58 | 638.1 | - |
| | 14 | 640 | 0.8 | - | 0 | 3.1 | 6.8 | 2.36 | 640.9 | - |
| | 15 | 725 | 0.91 | - | 1 | 2.6 | 6.5 | 4.68 | 622.9 | - |
| SFR-SCC | 16 | 620 | - | 593 | 0 | 4.6 | 8.9 | 0 | 626.1 | 64.9 |
| | 17 | 640 | - | 603 | 0 | 3.6 | 8.0 | 0 | 652.7 | 69.8 |
| | 18 | 665 | - | 660 | 0 | 3.4 | 8.6 | 4.79 | 612.9 | 57.0 |
| | 19 | 675 | - | 666 | 2 | 3.3 | 8.5 | 13.33 | 660.9 | 65.5 |
| | 20 | 690 | - | 680 | 2 | 2.9 | 7.0 | 17.56 | 606.1 | 58.9 |

$t_v$ = V-funnel flow time.

S% = percentage of segregation.

$f_{cu}$ = cube characteristic compressive strength.

$f_{ct}$ = splitting tensile strength.

For all tested mixes, decreasing w/cm ratio results in increasing of the compressive strength except for mixes 14 and 15 as shown in Fig. 3.f. This can be explained by the high dosage of HRWRA needed for these mixes to satisfy the fresh properties criteria. Table 4 and Fig. 6 demonstrate the gain of compressive strength for each mix comparing to its version with w/cm of 0.4. For mixes with sand/coarse aggregate ratio of 1.2, 1.1, and 0.9, the gain in compressive strength is higher between w/cm ratios of 0.4 and 0.38 than the gain between w/cm ratios of 0.38 and 0.35.

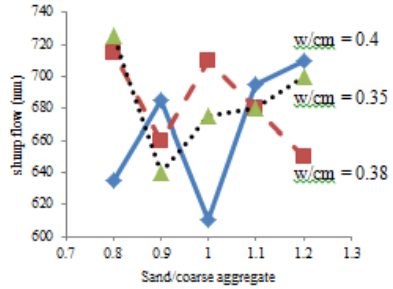


**Fig. 3. a.** Slump flow – sand/coarse aggregate relationship.

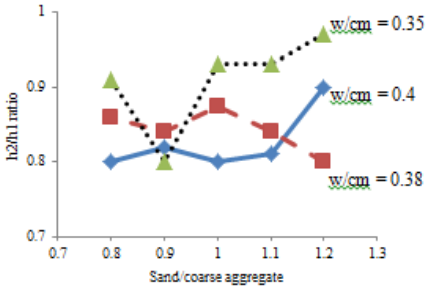


**Fig. 3. b.** $h_2/h_1$ ratio – sand/coarse aggregate relationship.

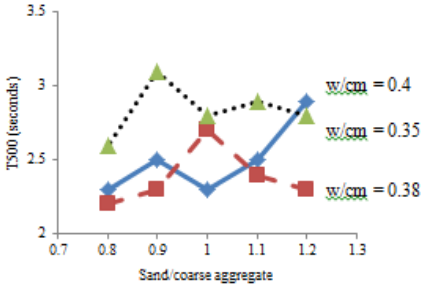


**Fig. 3. c.** T500 – sand/coarse aggregate relationship.

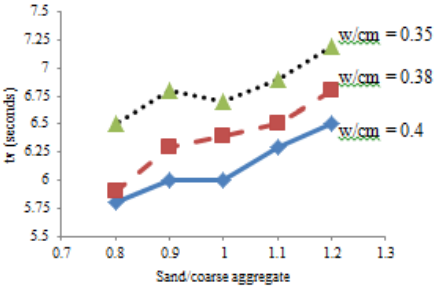


**Fig. 3. d.** $t_v$ – sand/coarse aggregate relationship.

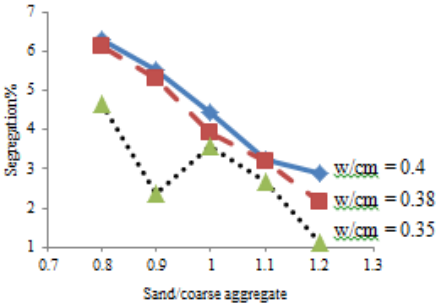


**Fig. 3. e.** Segregation% – sand/coarse aggregate relationship.

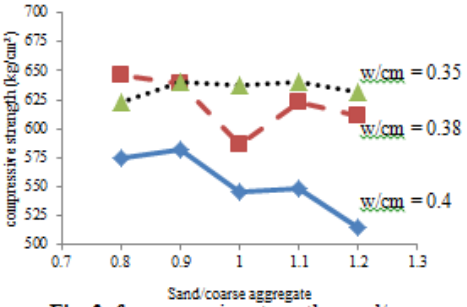


**Fig. 3. f.** compressive strength–sand/coarse aggregate relationship.

(a) Mix 1 (b) Mix 2 (c) Mix 3

(d) Mix 4 (e) Mix 5 (f) Mix 6

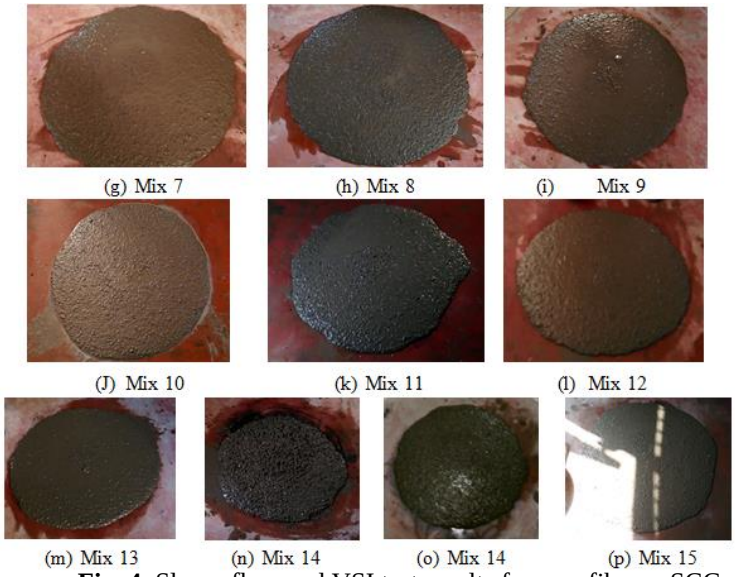


**Fig. 4.** Slump flow and VSI test results for non-fibrous SCC mixes.

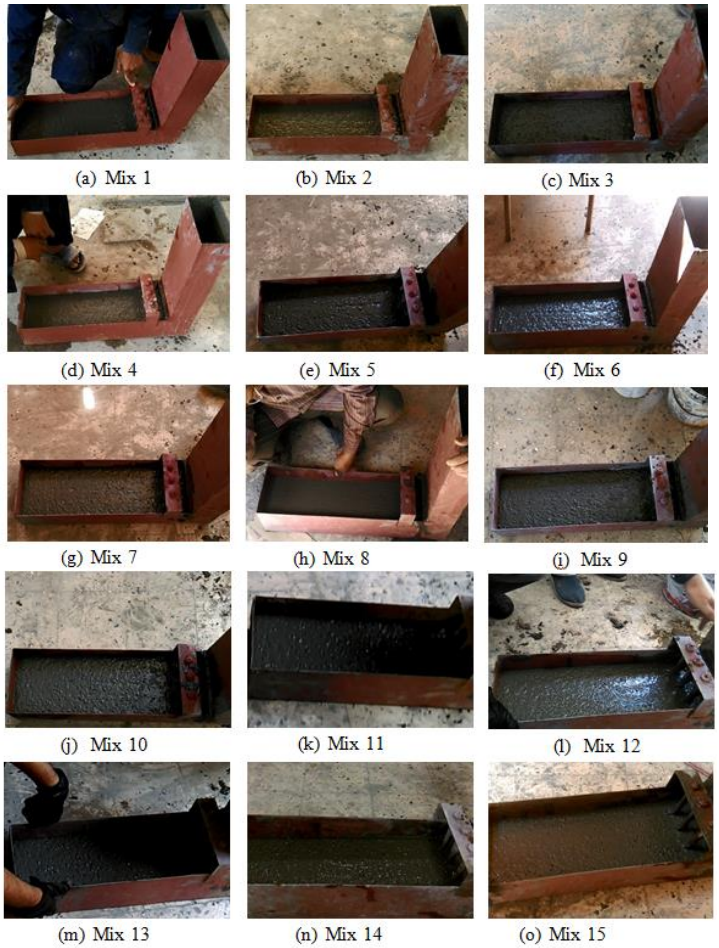


**Fig. 5.** L-box test results for non-fibrous SCC mixes.

**Table 4.**
percentage gain of compressive strength for non-fibrous SCC mixes.

| Mix No. | % gain of compressive strength | Mix No. | % gain of compressive strength |
|---|---|---|---|
| 6 | 18.56 | 11 | 22.71 |
| 7 | 13.73 | 12 | 17.03 |
| 8 | 7.25 | 13 | 16.83 |
| 9 | 9.83 | 14 | 10.15 |
| 10 | 12.35 | 15 | 8.31 |

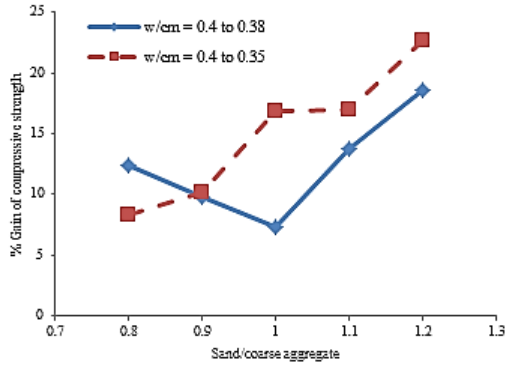


**Fig. 6.** %Gain of compressive strength – sand/coarse aggregate relationship.

### *3.2. SFR-SCC mixes*

It was necessary to increase the content of silica fume in order to enhance both the flowability and stability of this type of mixes. The crimped profile of the steel fibers significantly compromised the workability in such a way that basalt dust was crucial in order to provide a sufficient mortar volume to encapsulate both the coarse aggregate and the steel fibers. Fig. 7.a shows an earlier version of mix 16 before adding basalt dust. Clear segregation of coarse aggregate and steel fibers can be noticed. Figs. 7.b through 7.f show the mixes after utilization of basalt dust. Table 3 summarizes the test results of SFR-SCC mixes. It should be noted that the results shown in Table 3 are for the mixes developed using TYPE I cement with a grade of 32.5 N. Fig. 8.a shows that increasing sand/coarse aggregate ratio decreases both of slump and J-ring flow. T500 test results are consistent with slump flow's as shown in Figs. 8.a and 8.b. Figs. 8.a, 8.c and 8.d show the integration between flowability, passing ability (Δ) and stability for the SFRSCC mixes. Mixes 19 and 20 did not satisfy specification limits for segregation resistance as shown in Fig. 8.d, which is also characterized by the nesting of fibers around J-ring bars as shown in Figs.9.d and 9.e. A drop can be noticed in Figs. 8.a and 8.c for mix 17 implying low viscosity comparing to the trend of the curves. However, based on both the fresh and hardened properties, mix 17 is the best as it satisfies fresh properties criteria and has satisfactory compressive and tensile strengths as shown in Figs. 8.e and 8.f. The results of the mixes developed with the other types of cement are presented in Table 5. It's obvious that using TYPE I cement with a grade of 32.5 N had the best compressive and tensile strength for the different sand/coarse aggregate ratios. Also, the fineness of the TYPE I cement with a grade of 42.5 N was not constant for all batches. This was evident in the large increase of slump flow for some mixes such as mix 17 and 19 and the decrease of their compression

and tensile strength compared to the mixes developed with the first type. For the mixes developed with TYPE II cement with a grade of 52.5 N the compression and tensile strength were either equal to or less than the values for the mixes developed with the first type. Neither grade 42.5 N cement nor grade 52.5 N cement changed the fact that mix 19 did not satisfy the specification limits for percentage segregation. That's why mix 20 was not needed to be tested for these types of cement.

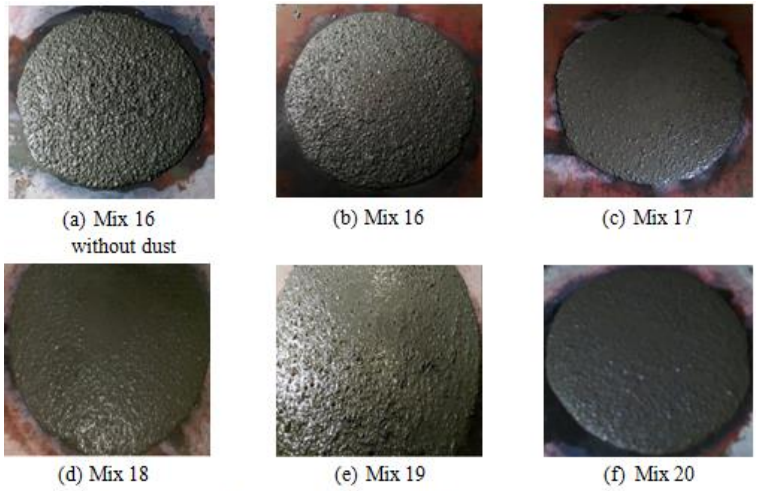

(a) Mix 16 without dust (b) Mix 16 (c) Mix 17

(d) Mix 18 (e) Mix 19 (f) Mix 20

Fig. 7: Slump flow and VSI test results for SFR-SCC mixes.

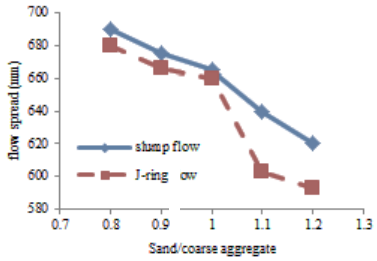


**Fig. 8. a.** Slump flow & J-ring flow – sand/coarse aggregate relationship.

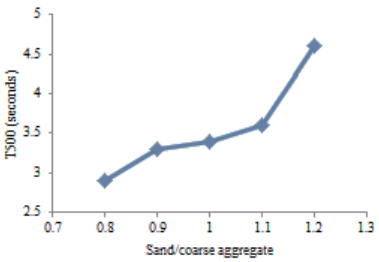


**Fig. 8. b.** T500 – sand/coarse aggregate relationship.

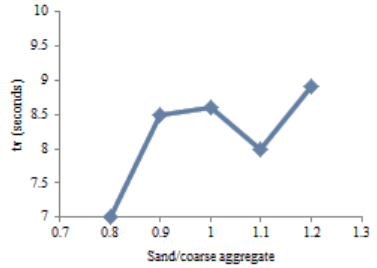


**Fig. 8. c.** $t_v$ – sand/coarse aggregate relationship.

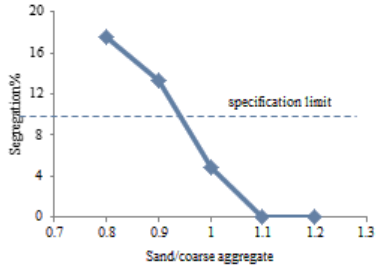


**Fig. 8. d.** Segregation% – sand/coarse aggregate relationship.

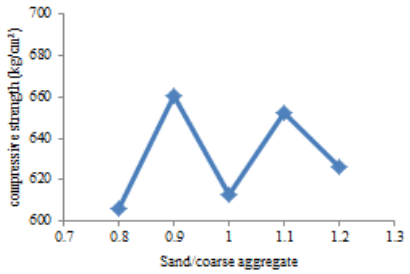


**Fig. 8. e.** Compressive strength – sand/coarse aggregate relationship.

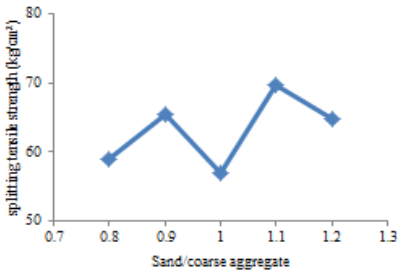


**Fig. 8. f.** Splitting tensile strength – sand/coarse aggregate relationship.

(a) Mix 16

(b) Mix 17

(c) Mix 18

(d) Mix 19

(e) Mix 20

Fig. 9: J-ring flow test results for SFR-SCC mixes.

**Table 5.**
Test results for tested mixes with different types of cement.

| Mixture type | Mixture No. | Slump flow (mm) | J – ring flow (mm) | VSI | $t_v$ (sec) | S% | $f_{cu}$ (kg/cm$^2$) | $f_{ct}$ (kg/cm$^2$) |
|---|---|---|---|---|---|---|---|---|
| SFR-SCC | TYPE I cement with a grade of 32.5 N | | | | | | | |
| | 16 | 620 | 593 | 0 | 8.9 | 0 | 626.1 | 64.9 |
| | 17 | 640 | 603 | 0 | 8.0 | 0 | 652.7 | 69.8 |
| | 18 | 665 | 660 | 0 | 8.6 | 4.79 | 612.9 | 57.0 |
| | 19 | 675 | 666 | 2 | 8.5 | 13.33 | 660.9 | 65.5 |
| | TYPE I cement with a grade of 42.5 N | | | | | | | |
| | 16 | 618 | 569 | 0 | 8.7 | 1.2 | 595.2 | 63.0 |
| | 17 | 700 | 670 | 0 | 7.9 | 0 | 645.1 | 65.7 |
| | 18 | 653 | 604 | 0 | 8.7 | 5.16 | 590.5 | 55.2 |
| | 19 | 720 | 698 | 2 | 7.4 | 16.23 | 643.4 | 65.5 |
| | TYPE II cement with a grade of 52.5 N | | | | | | | |
| | 16 | 600 | 594 | 0 | 9.0 | 0 | 644.1 | 64.9 |
| | 17 | 623 | 588 | 0 | 7.8 | 0 | 649.2 | 66.9 |
| | 18 | 655 | 618 | 0 | 8.4 | 5.04 | 579.2 | 52.3 |
| | 19 | 683 | 651 | 2 | 8.1 | 14.68 | 639.5 | 60.8 |

$t_v$ = V-funnel flow time.
S% = percentage of segregation.
$f_{cu}$ = cube characteristic compressive strength.
$f_{ct}$ = splitting tensile strength.

## 4. An application of the produced repairing mixes

To investigate the efficiency of the suggested SFR-SCC mix for repairing, two reinforced concrete beams (B0) and (B1) designed to fail in shear were cast using normal strength concrete with characteristic strength 200 kg/cm$^2$. Fig. 10.a shows the details of reinforcement of the tested beams. Beam (B0) had a cross section of 120x300 mm, span = 1620 mm, shear span = 540 mm with a/d ratio of 2.0. It was reinforced with 2Φ10 mm as stirrup hanger, 2Φ16 mm as longitudinal flexural reinforcement and stirrups Φ6 mm with spacing of 200 mm as web reinforcement. Beam (B0) had neither shear connectors nor SFR-SCC jacket, and was tested after 28 days under three point loading up to failure as a control beam. The other beam (B1) had a cross section of 120x300 mm, span = 1620 mm, shear span = 540 mm with a/d ratio of 2.0. It was reinforced with 2Φ10 mm as stirrup hanger, 2Φ16 mm as longitudinal flexural reinforcement and stirrups Φ6 mm with spacing of 200 mm as web reinforcement. It was loaded up to the first shear cracking. Then both the bottom and sides surfaces were prepared by a grinding disc and drilled to insert shear connectors with 4 mm diameter as shown in Fig. 10.b with an adhesive mortar. Before casting a U-shaped SFR-SCC jacket with 30 mm thickness using mix17, a modified epoxy resin-based adhesive was applied to the sides and bottom of the beam. Then the repaired beam (B1) was tested after 28 days under three-point loading up to failure [2]. Tests were conducted using EMS hydraulic machine with 60 tons capacity with the aid of computerized data acquisition system.

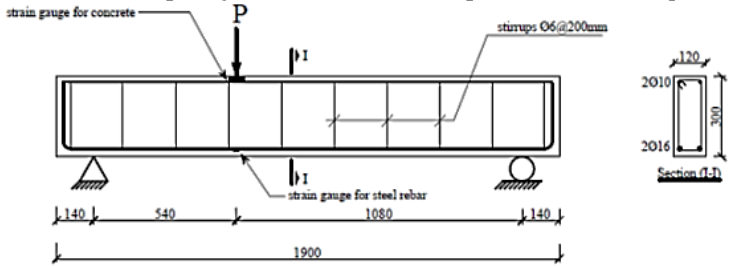


**Fig. 10. a.** Details of reinforcement for tested beams (Dimensions in mm).

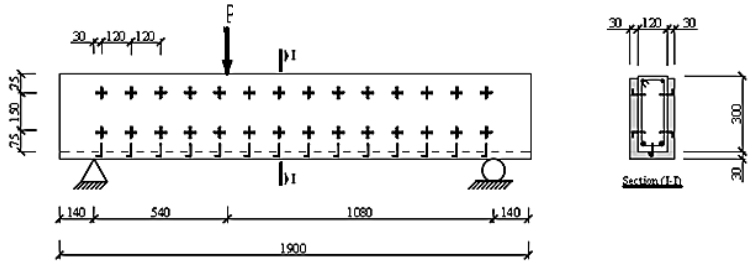


**Fig. 10. b.** Beam (B1) at repairing process (Dimensions in mm).

## 5. Results and discussion of the tested beams

Fig. 11.a and 11.c showed that beam (B0) exhibited a shear-compression failure while beam (B1) exhibited a diagonal-tension failure. The SFR-SCC jacket was found to be beneficial, increasing the cracking load from 4.0 tons for beam (B0) to 7.5 tons for beam (B1), and increasing the ultimate load from 8.85 tons for beam (B0) to 16.9 tons for beam (B1). The jacket also reduced the number of cracks and the mode of failure was more ductile for the repaired beam comparing to beam (B0).

Fig.12.a. shows that repairing with SFR-SCC significantly enhanced the flexural stiffness for beam (B1) in both pre-cracking and post-cracking stages, comparing to beam (B0). Such increase was found for RC beams when longitudinal steel and/or concrete strength was increased rather than increasing the effective depth of the beam [7]. As presented in neither Fig. 12.b, neither beam (B0) nor (B1) has reached the specified crushing strain of 0.003 by many codes. Beam (B1) exhibited more compressive strain than (B0) at failure. However, for the same load, the repaired beam (B1) exhibited less compressive strain than beam (B0), indicating the contribution of SFR-SCC in the compression zone of the repaired beam (B1). Also, in Fig. 12.c, for the same load the repaired beam (B1) exhibited less steel rebars' tensile strain than beam (B0), indicating the contribution of SFR-SCC in the tension zone of the beam (B1). For the beam (B1) after reaching 10 tons, the tensile strain increased at a lower rate indicating more tensile stresses carried by SFR-SCC at this stage. Table 6 shows cracking loads, ultimate loads, maximum deflections and maximum measured strains for beams (B0) and (B1).

**Table 6.**

Cracking loads, ultimate loads, maximum deflections and maximum measured strains for tested beams.

| Beam | $P_{cr}$ (ton) | $P_u$ (ton) | $f_{cu}$ (kg/cm$^2$) | $f_{cu}$' (kg/cm$^2$) | $f_{ct}$' (kg/cm$^2$) | $\delta_{max}$ (mm) | $\varepsilon_{c\,max}$ (με) | $\varepsilon_{s\,max}$ (με) |
|---|---|---|---|---|---|---|---|---|
| BO | 4.0 | 8.85 | 224.8 | - | - | 5.14 | 1076 | 1532 |
| BA1 | 7.5 | 16.9 | 220.7 | 655.8 | 72.1 | 6.64 | 1340 | 1823 |

| Beam | $P_{cr\,B1}$ /$P_{cr\,B0}$ | $P_{u\,B1}$ /$P_{u\,B0}$ | $\delta_{max\,B1}$ /$\delta_{max\,B0}$ | $\varepsilon_{c\,max\,B1}$ /$\varepsilon_{c\,max\,B0}$ | $\varepsilon_{s\,max\,B1}$ /$\varepsilon_{s\,max\,B0}$ |
|---|---|---|---|---|---|
| BO | - | - | - | - | - |
| BA1 | 1.875 | 1.91 | 1.29 | 1.25 | 1.19 |

$P_{cr}$ = Inclined cracking load.
$P_u$ = Ultimate load.
$f_{cu}$ = cube characteristic compressive strength of the RC beam.
$f_{cu}$' = cube characteristic compressive strength of the SFR-SCC jacket.
$f_{ct}$' = splitting tensile strength of the SFR-SCC jacket.
$\delta_{max}$ = Maximum deflection.
$\varepsilon_{c\,max}$ = Maximum compressive strain for concrete.
$\varepsilon_{s\,max}$ = Maximum tensile strain for steel.

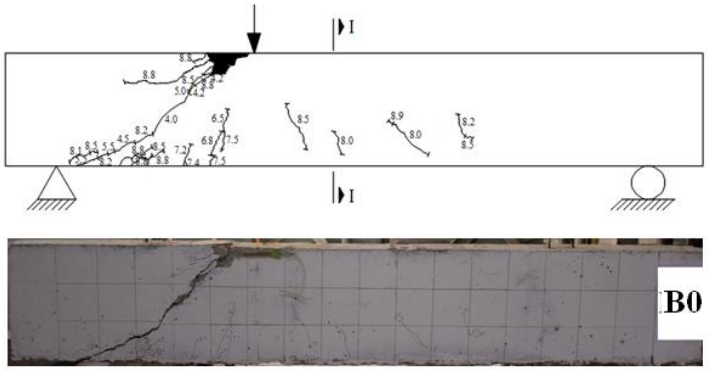


**Fig. 11. a.** Cracking pattern and mode of failure for beam (B0).

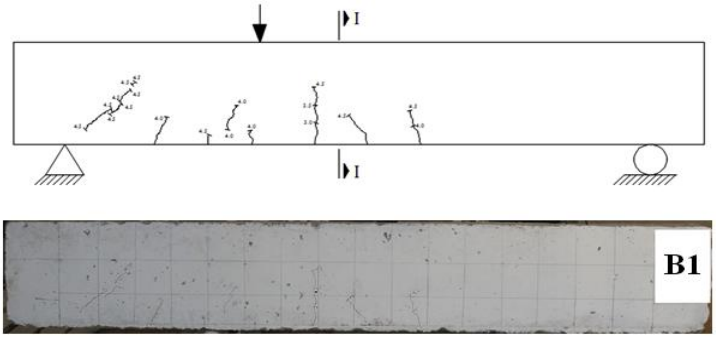


**Fig. 11. b.** Cracking pattern for beam (B1) before repairing.

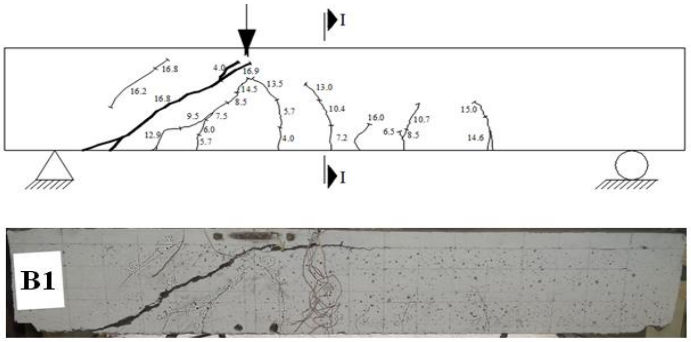


**Fig. 11. c.** Cracking pattern and mode of failure for beam (B1) after repairing.

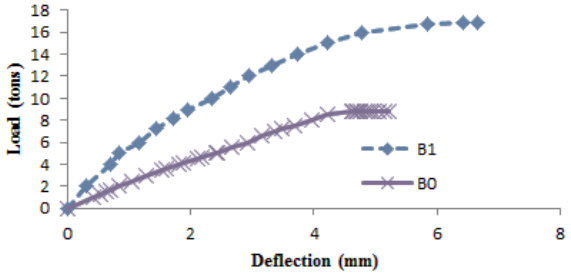


**Fig. 12. a.** Load-deflection relationships for the tested beams.

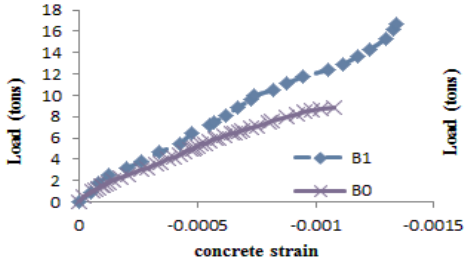


**Fig. 12. b.** Load- compressive strain relationships for the tested beams.

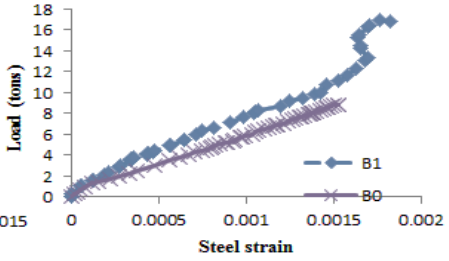


**Fig. 12. c.** Load- tensile strain relationships for the tested beams.

## 6. Conclusions

Based on the test results and the pre-mentioned discussion, the following conclusions can be drawn:

1- For the non-fibrous SCC mixes, increasing the sand/coarse aggregate ratio can significantly enhance the stability of the mix. However, the compressive strength does not increase in the same manner.

2- Using of filler such as basalt dust is necessary for the non-fibrous SCC mixes with low sand/coarse aggregate ratio such as 0.9 and 0.8 at w/cm ratio of 0.35 in order to maintain the desired stability of the mix.
3- The addition of crimped steel fibers to self-consolidating concrete mixes can significantly alter their fresh properties.
4- Basalt dust was found to be necessary for SFR-SCC mixes to increase mortar volume to effectively encapsulate both coarse aggregate and the crimped steel fibers. However, it was found that for low sand/coarse aggregate ratio such as 0.9 and 0.8 with 0.75% volume fraction of crimped steel fibers, the stability criteria could not be achieved. These low sand/coarse aggregate ratios may be used only with low volume fractions of straight steel fibers with crimped ends [3].
5- A suitable mix is obtained with sand/coarse aggregate ratio of 1.1. This mix had a slump flow diameter of 640 mm, a J-ring flow diameter of 603 mm, and zero segregation percentage. It had also compressive and splitting tensile strengths equal 652 and 69.8 kg/cm$^2$, respectively. These results were found satisfactory for both fresh and hardened properties criteria.
6- The used repairing technique increased the cracking and ultimate loads of the repaired beam comparing to the control beam by 87.5% and 91%, respectively.
7- The load-deflection relationships showed a significant increase in the flexural stiffness for the repaired beam. The applied repairing technique also changed the mode of failure from shear-compression failure to diagonal-tension failure.
8- At the same load, the repaired beam (B1) exhibited less deflection, compressive and tensile strain than beam (B0). This ensures the great contribution of the SFR-SCC jacket in bearing the applied stresses.

## REFERENCES

[1] Alyousif, R (2010). "Design and Testing of Fiber Reinforced Self Compacting Concrete". MSc Thesis, Eastern Mediterranean University, Gazimağusa, North Cyprus.
[2] Arafa, A., (2012). "Strengthening and Repair of R.C Beams Subjected to Short Time Repeated Load by Using Steel Fiber Concrete Jacket". MSc Thesis, Assiut University, Assiut, Egypt.
[3] Deeb, R.. Ghanbari, A., and Karihaloo, B.L. (2012). "Development of self-compacting high and ultra-high performance concretes with and without steel fibers". *Cement & Concrete Composites*, 34, 185–190.
[4] Gonzalo Ruano, Facundo Isla, Rodrigo Isas Pedraza, Domingo Sfer, and Bibiana Luccioni (2014). "Shear retrofitting of reinforced concrete beams with steel fiber reinforced concrete". *Construction and Building Materials*, 54, 646–658.
[5] Grünewald, S., Walraven, J.C. (2003). "Rheological measurements on self-compacting fibre reinforced concrete". In: Wallevik Ó, Níelsson I, editors. Proceedings of the 3rd international RILEM symposium on self-compacting concrete, S.A.R.L France; 2003. p. 49–58.
[6] Grünewald, S., and Walraven, J. C. (2010). "Maximum Fiber Content and Passing Ability of Self-Consolidating Fiber-Reinforced Concrete". *ACI Special Publication*, 274(2), 15-30.
[7] Mahmoud, K., and El-Salakawy, E. (2016). "Size Effect on Shear Strength of Glass Fiber-Reinforced Polymer-Reinforced Concrete Continuous Beams". *ACI Structural Journal*, 113(1).
[8] Oliveira, F., (2010). "Design-oriented constitutive model for steel fiber reinforced concrete". PhD Thesis, Universitat Politècnica de Catalunya, Spain.
[9] Spangenberg J, Roussel N, Hattel JH, Thorborg J, Geiker MR, Stang H, et al. Prediction of the impact of flow-induced in homogeneities in self-compacting concrete (SCC). In: Khayat KH, Feys D, editors. Proceedings of the 2010 international RILEM symposium on self-compacting concrete. Design, production and placement of self-consolidating concreteeds, Canada; 2010. p. 209–14.

# تطوير الخرسانة ذاتية الدمك المسلحة بألياف الصلب لأغراض الترميم

**الملخص العربى:**

تتعرض بعض العناصر الإنشائية للشروخ نتيجة عدد من العوامل مثل أخطاء التصميم و التنفيذ أو زيادة الأحمال الواقعة على هذه العناصر عن الأحمال التصميمية لها, مما يتطلب إصلاح هذه العناصر. و توجد العديد من طرق إصلاح العناصر الإنشائية مثل القمصان الخرسانية المسلحة و التدعيم بواسطة البوليمرات المسلحة بالألياف و ألواح الحديد. لكن الإصلاح و الترميم بواسطة الخرسانة ذاتية الدمك المسلحة بألياف الصلب يتميز بالعديد من المزايا عما سبق من أساليب الترميم. حيث أنه أكثر كفاءة في مقاومة الحريق مقارنة بالبوليمرات المسلحة بالألياف وأكثر مقاومة للصدأ من ألواح الحديد و أقل سمكاً و وزناً من قمصان الخرسانة المسلحة. بالإضافة إلى خصائص الخرسانة الذاتية الدمك التي تمكّن من ترميم المنشآت بقمصان ذات سمك صغير.

و من ثم كان الهدف من هذا البحث تطوير خلطات خرسانية ذاتية الدمك مسلحة بألياف الصلب ذات الشكل المتعرج بكامل الطول للإستفادة من الخصائص الميكانيكية العالية لهذا النوع من الألياف مع الخرسانة الذاتية الدمك في أغراض إصلاح و ترميم الكمرات الخرسانية التي بها شروخ ناتجة من إجهادات القص. و لهذا الغرض تم اختبار خمسة عشر خلطة خرسانية ذاتية الدمك بدون ألياف و من ثم خمسة خلطات خرسانية ذاتية الدمك مسلحة بألياف الصلب ذات الشكل المتعرج بكامل الطول. و كانت المتغيرات التي تم دراستها نسبة المياه إلى المواد الأسمنتية, نسبة الرمل إلى الركام الخشن و استخدام البازلت المطحون في الخلطة الخرسانية. و أوضحت النتائج التي تم الحصول عليها أن تحقيق معايير قابلية السريان تكفي لتصميم الخلطات الخرسانية ذاتية الدمك بدون ألياف. بينما ينبغي تحقيق كلاً معايير السريان و قابلية المرور لتصميم الخلطات الخرسانية ذاتية الدمك المسلحة بألياف الصلب ذات الشكل المتعرج. كما وجد أن استخدام البازلت المطحون لا غنى عنه في الخلطات الخرسانية ذاتية الدمك بدون ألياف ذات النسب الصغيرة للرمل إلى الركام الخشن مثل 0.8 و 0.9. كما وجد أنه ضروري للخلطات الخرسانية ذاتية الدمك المسلحة بألياف الصلب ذات الشكل المتعرج بصفة عامة. كما تم الحصول على خلطة خرسانية ذاتية الدمك مسلحة بألياف الصلب ذات نتائج مرضية على صعيديّ خواص الخرسانة الطازجة و المتصلدة و ذلك عند نسبة رمل إلى الركام الخشن 1.1. بينما فشلت الخلطات المسلحة بالألياف عند نسبتي الرمل إلى الركام الخشن 0.8 و 0.9 في تحقيق حدود المواصفات لخواص الخرسانة الطازجة.

و للتحقّق من كفاءة الخلطة التي تم الحصول عليها تم إستخدامها في عمل قميص لإصلاح كمرة تكوّن بها شروخ قصيّة. و من أجل هذا الغرض تم صب و اختبار كمرتين متماثلتين من الخرسانة المسلحة تحت نظام تحميل استاتيكي ثلاثي النقاط. أحد الكمرتين تم اختبارها ككمرة مرجعية بينما الكمرة الأخرى تم إصلاحها باستخدام الخلطة الخرسانية ذاتية الدمك المسلحة بألياف الصلب التي تم الحصول عليها. هذا و قد أوضحت النتائج أن حمل الشرخ القصي و حمل الإنهيار قد زادا بنسبة 87.5% و 91% على الترتيب بالمقارنة بالكمرة المرجعية. أيضاً تم تحسين صلابة الكمرة التي تم إصلاحها ضد إجهادات الإنحناء بشكل فعال بالمقارنة بالكمرة المرجعية. كما بيّنت نتائج الاختبار فعالية مشاركة الخرسانة ذاتية الدمك المسلحة بألياف الصلب في كلاً منطقتي الشد و الضغط للكمرة التي تم إصلاحها.